

# Journal of Biomedical Optics

BiomedicalOptics.SPIEDigitalLibrary.org

## ***In vivo* studies of ultrafast near-infrared laser tissue bonding and wound healing**

Vidyasagar Sriramoju  
Robert R. Alfano

# *In vivo* studies of ultrafast near-infrared laser tissue bonding and wound healing

Vidyasagar Sriramoju and Robert R. Alfano\*

The City College of New York, Institute of Ultrafast Spectroscopy and Lasers, Department of Physics and Electrical Engineering, 160 Convent Avenue, New York, New York 10031, United States

**Abstract.** Femtosecond (fs) pulse lasers in the near-infrared (NIR) range exhibit very distinct properties upon their interaction with biomolecules compared to the corresponding continuous wave (CW) lasers. Ultrafast NIR laser tissue bonding (LTB) was used to fuse edges of two opposing animal tissue segments *in vivo* using fs laser photoexcitation of the native vibrations of chromophores. The fusion of the incised tissues was achieved *in vivo* at the molecular level as the result of the energy–matter interactions of NIR laser radiation with water and the structural proteins like collagen in the target tissues. Nonthermal vibrational excitation from the fs laser absorption by water and collagen induced the formation of cross-links between tissue proteins on either sides of the weld line resulting in tissue bonding. No extrinsic agents were used to facilitate tissue bonding in the fs LTB. These studies were pursued for the understanding and evaluation of the role of ultrafast NIR fs laser radiation in the LTB and consequent wound healing. The fs LTB can be used for difficult to suture structures such as blood vessels, nerves, gallbladder, liver, intestines, and other viscera. Ultrafast NIR LTB yields promising outcomes and benefits in terms of wound closure and wound healing under optimal conditions. © 2015 Society of Photo-Optical Instrumentation Engineers (SPIE) [DOI: [10.1117/1.JBO.20.10.108001](https://doi.org/10.1117/1.JBO.20.10.108001)]

**Keywords:** laser tissue bonding; laser surgery; near-infrared laser welding; femtosecond laser tissue bonding; nonlinear photo absorption in proteins; ultrafast lasers on wound healing; *in vivo* ultrafast laser studies; nonthermal laser effects.

Paper 150412R received Jun. 18, 2015; accepted for publication Aug. 28, 2015; published online Oct. 14, 2015.

## 1 Introduction

Laser tissue binding (LTB) is a promising state-of-the-art alternative method to wound repair over using conventional techniques such as sutures, staples, and clips.<sup>1–3</sup> The salient properties of laser light wavelength, polarization, and pulse duration can be adjusted to optimize the efficacy of tissue binding. LTB has potential advantages in most branches of surgery for its rapid wound healing, reduced surgical time, less foreign body reactions, very minimal fibrosis, and negligible chances for development of strictures or stenosis. The other advantages of LTB include immediate intraoperative watertight sealing and minimal scar tissue formation over conventional wound closure methods.<sup>4–6</sup> Wounds treated by femtosecond (fs) LTB have minimal inflammatory response, near-normal collagen content, minimal breaks, and less disorientation in the organization of tissue collagen and elastin fibers. The ultrafast light pulse duration and wavelengths that match the absorption modes of covalent and noncovalent bonds of the native tissue chromophores are the key factors behind a nonequilibrium nonthermal state of tissue. The excited vibrational modes of water and collagen cause transient disruption and are followed immediately by the reformation of the disrupted bonds. A chromophore is defined as “the part of a molecular entity consisting of an atom or group of atoms in which the electronic transition responsible for a given spectral band is approximately localized.”<sup>7</sup>

The LTB procedure typically involves illuminating the reapproximated edges of a bisected tissue with a laser beam at an

appropriate wavelength which is absorbed by the molecules in the tissue. The scattering length and absorption coefficient of the tissue determine the penetration depth of the light, and hence, the thickness of the weld can be attained. Optimum tissue fusion is achieved when the laser penetration depth matches the thickness of the tissue to be welded. In this research study, fs near-infrared (NIR) laser beam at 1550 nm was used *in vivo* in guinea pigs to excite vibration combinations of water and collagen in the surgically incised tissues for inducing the formation of bonds and fusing tissues together; no extrinsic materials were used for enhancing or inducing tissue bonding. The key features of NIR LTB are summarized in Table 1.

The types of tissues that will be fused and the areas of surgery that will be impacted are (a) vascular surgery—coronary arterial surgery, repair of trauma to veins and arteries, arteriovenous shunt, and intracranial vascular surgery; (b) general, skin, and plastic surgeries, surgical incision, lacerations from trauma with reduced scarring; (c) surgical procedures involving gastrointestinal system and viscera like lung, liver, and kidney; and (d) ocular surgeries. The major molecules involved in tissue molecular cross-linking in these tissues are water and structural proteins collagen and elastin.

The strength (tensile strength/breaking strength) of welded tissue has been a major limitation to clinical application. A zero time tensile strength of 0.5 kg/cm<sup>2</sup> or less is typical when continuous wave (CW) lasers are used.<sup>4</sup> The tensile strengths that we achieved with minimal damage and full thickness welds are far better in this regard (1.13 ± 0.27 kg/cm<sup>2</sup> for human aorta, 1.33 ± 0.15 kg/cm<sup>2</sup> for porcine aorta, and

\*Address all correspondence to: Robert R. Alfano, E-mail: [ralfano@sci.cuny.edu](mailto:ralfano@sci.cuny.edu)

**Table 1** The cardinal features of fs near-infrared (NIR) laser tissue bonding (LTB).

The cardinal features of NIR LTB using 1550 nm fs pulse laser	
1	The penetration depth can be controlled by tuning the laser wavelength so that the water absorption coefficient matches the desired penetration depth
2	Use of 100 fs pulses can invoke nonthermal mechanisms, such as electronic or vibrational processes and thereby reduce collateral damage to surrounding tissue, while producing stronger bonding
3	Immediate water-tight seal is formed
4	Reduction in surgical time, very distinct pattern of wound healing with less scar tissue formation
5	Reduced risk of foreign body reaction and minimal chances of local toxic reactions
6	Reduction in infection chances, intensity of inflammatory response, and immune reaction

1.05 ± 0.19 kg/cm<sup>2</sup> for human skin). These values are two times greater than those from tissue immediately after suture removal.<sup>8</sup>

LTB using CW laser beam involves the partial denaturation and renaturation of collagen by thermal mechanisms that result from the laser-tissue interaction.<sup>1</sup> During bonding, water in the tissue absorbs the laser energy and subsequently heats the collagen helix. When the collagen tissue temperature rises above 60°C, H-bonding, hydrophobic interactions, and electrostatic interactions are disrupted and partial dissociation collagen triple helix occurs transiently. This is followed by reformation of the same bonding of the tissue protein molecules as the tissue cools (Fig. 1). Collagen is the main structural protein of the body. The collagen molecules, after secretion by the cells, assemble into characteristic fibers responsible for the functional integrity of tissues, such as skin, cornea, bone, cartilage, and tendon.<sup>9</sup> They contribute a structural framework to other tissues, such as blood vessels and most organs. Cross-links between adjacent molecules are a prerequisite for the collagen fibers to withstand

the physical stresses to which they are exposed. Collagen forms a triple helical structure.<sup>9</sup> Every third amino acid is glycine (Gly), and a high proportion of the remaining residues are proline (Pro) and hydroxyproline (Hyp).<sup>10</sup> The most common triplet combination in collagen is Gly-Pro-Hyp. The Hyp residue's hydroxyl group was shown to increase the thermal stability of the triple helix.<sup>11</sup> Direct pumping of collagen in NIR in 1700 to 2500 nm can occur.

A diagram of the different water mediated bonds of the collagen chains, modified from the work of Brodsky and Ramshaw,<sup>10</sup> is shown in Fig. 2. Hydration is thought to play an important role in maintaining the collagen helical structure.<sup>12</sup> Interstitial water is separated into two distinct classes: tightly bound and free water.<sup>13</sup> The bound water stabilizes the collagen helix. Water mediated H-bonding is found in intrachain and interchain bonds linking two carbonyl groups [CO(Hyp)—H<sub>2</sub>O—CO(Gly)]; or OH groups to carbonyl groups [OH—H<sub>2</sub>O—CO(Gly) or OH—H<sub>2</sub>O—CO(Hyp)].<sup>9</sup> The bound water maintains the distance between the chains and prevents collapse of the collagen helix. The left side of Fig. 2 shows direct H-bonding in the helix while the middle and right sides show water (indicated by w in Fig. 2) mediated intrachain (between amino acids on the same chain) and interchain (between amino acids on different chains) hydrogen bonding. The water maintains the structure and spacing of helices as well as the chains. Photo excitation of the O—H stretch vibrations of the water molecules with picosecond (ps) and fs pulses may weaken the intrachain and interchain bonds until the water molecules relax. While vibrational modes are excited, the water molecules may become mobile and move along the helix. The relaxation lifetimes of the optical excited vibrations are on the order of 3 ps.<sup>14,15</sup>

An explanation for the stability of the collagen molecules is suggested in the works by Holmgren et al.<sup>16,17</sup> and Brodsky et al.<sup>10,18,19</sup> as depicted on Fig. 2. The thermal stability of collagen's triple helix was noted to be enhanced by the OH group on the pyrrolidine ring of hydroxyproline.<sup>11</sup> This would involve direct interchain H-bonding. This stability was ascribed to a network of bridging water molecules,<sup>9</sup> detected by x-ray diffraction analysis of crystalline collagen.<sup>18</sup> However, Holmgren et al. believe that water bridges are not likely to contribute to collagen's stability,<sup>17</sup> as the entropic cost of building and maintaining the water bridges would be enormous.<sup>20</sup> They calculate that the

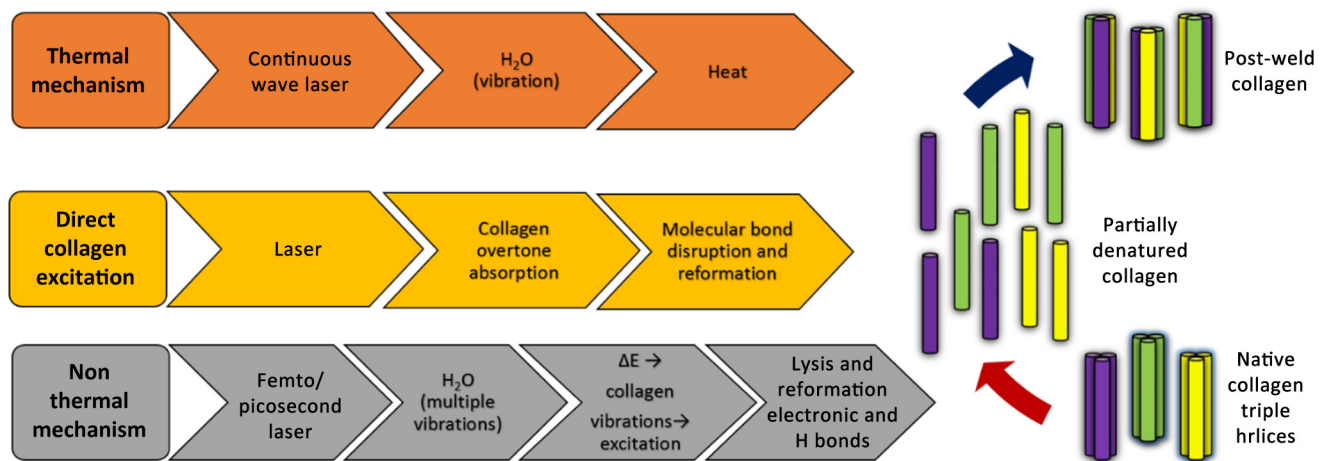


**Fig. 1** Energy transfer mechanisms of laser-tissue interactions during continuous wave (CW) and femto-second (fs)/ps near-infrared (NIR) welding.

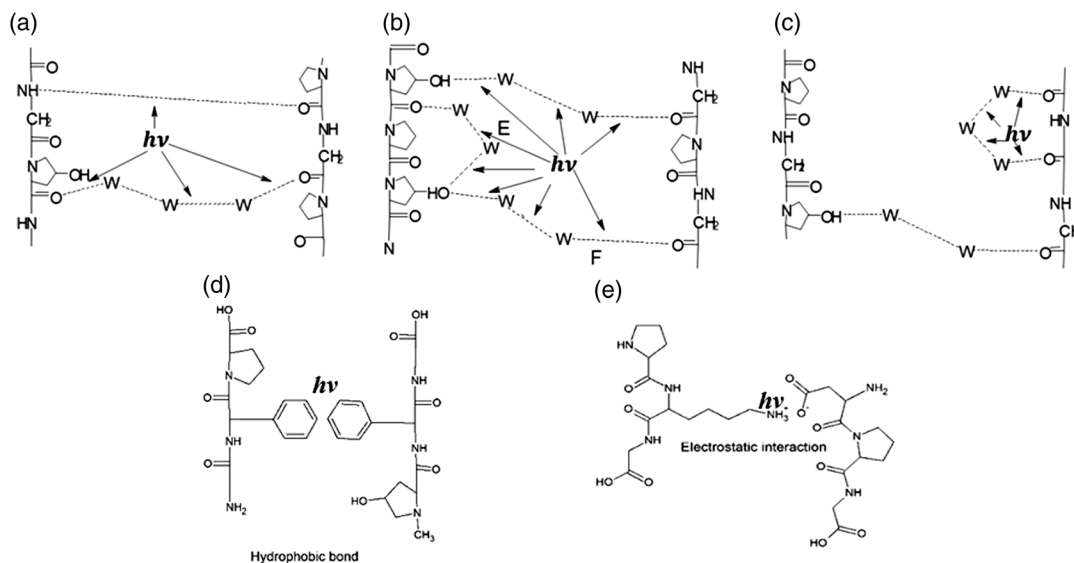


**Fig. 2** Different types of bonds stabilizing the collagen triple helix: (a–c) hydrogen bonds, (d) hydrophobic bond, and (e) electrostatic interaction.

bridges would require more than 500 water molecules per triple helix. They note that electron-withdrawing groups can alter the attributes of molecules<sup>21</sup> and that the inductive effect of the OH group of hydroxyproline is apparent in the structure<sup>22</sup> and properties of molecules that mimic collagen.<sup>23</sup> Under these circumstances, the water molecules may serve as a transfer agent, absorbing energy from the laser and transferring it to the collagen, disrupting the stabilizing inductive effects.

The key process in LTB is the NIR absorption by photoexcitation of vibration states due to combination vibration modes of molecules (Figs. 1, 4, and 5). The three primary vibrational energies of water responsible for overtone and combination absorption are: the OH symmetric stretching mode,  $\nu_1$  at  $3500\text{ cm}^{-1}$ ; the OH bending mode,  $\nu_2$  at  $1598\text{ cm}^{-1}$ ; and the asymmetric OH stretching mode,  $\nu_3$  at  $3290\text{ cm}^{-1}$ . Changes in separation between collagen helices are reflected in the Raman spectra of O–H and N–H vibrational bands in the  $3100$  to  $3800\text{ cm}^{-1}$  range.<sup>24</sup> Excitations in  $\text{H}_2\text{O}$  molecules may excite collagen and hydrogen bonding bands. The  $\nu_2$  bending mode of water is near resonant with the amide I band of collagen allowing for efficient energy transfer between these two modes. The lifetime of the vibrational state in liquid water is on the order of 3 ps, and is somewhat longer in a bound state.<sup>14,15</sup> The combination modes (1,1,1) are responsible for  $\text{H}_2\text{O}$  absorption at  $1064\text{ nm}$  and the combination mode (1,0,1) is responsible for  $\text{H}_2\text{O}$  absorption at  $1550\text{ nm}$ . The  $1550\text{ nm}$  wavelength is selected for the fs laser for this study. The Raman spectrum of collagen in the aorta has been studied extensively<sup>24–27</sup> and assignments have been made for the vibrations observed. The key modes and associated frequencies are: amide I,  $1660\text{ cm}^{-1}$ ; C=C bending of phenylalanine at  $1591\text{ cm}^{-1}$ ,  $\text{CH}_2$  bending mode of proteins at  $1458\text{ cm}^{-1}$ ,  $\text{CH}_3\text{CH}_2$  twisting mode at  $1321\text{ cm}^{-1}$ , amide III at  $1277\text{ cm}^{-1}$ , C–N stretching mode at  $1123\text{ cm}^{-1}$ , ring breathing mode of phenylalanine at  $1014\text{ cm}^{-1}$ , C–C stretching mode of proline at  $935\text{ cm}^{-1}$ , C–C stretch of hydroxyproline at  $868\text{ cm}^{-1}$ , and C–H in-plane bending mode at  $722\text{ cm}^{-1}$ . The water molecules forming hydrogen bonds in collagen result in progressively increasing amide A absorption bands at

$3320\text{ cm}^{-1}$  (–OH) that correspondingly increase with collagen humidity.<sup>28</sup> This band results in the first overtone absorption at  $6640\text{ cm}^{-1}$  ( $1506\text{ nm}$ ).

An erbium-doped Raman-shifted fs fiber laser (IMRA femtolite)  $1550\text{ nm}$  beam with  $\leq 100\text{ fs}$  pulse width and  $75\text{ MHz}$  repetition rate was delivered in a noncontact method to surgically incised tissues. The laser beam was focused with a short focal length lens ( $f = 70\text{ mm}$ ) producing a spot size of  $100\text{ }\mu\text{m}$ , positioned at  $50\text{ mm}$  from the lens. The wavelength was measured with a spectrometer and the power output of the focus lens was measured with a power meter. The power output was kept under  $220\text{ mW}$ . The power density was  $175\text{ W/cm}^2$ . Collateral thermal damage to the surrounding tissue is a concern during bonding. Results of our measurements demonstrate that thermal damage is a more significant issue for laser surgical procedures. Thermal damage to aorta and skin tissue occurs with CW NIR lasers at high power as a result of welding.<sup>29,30</sup> Previous skin welding studies have used CW delivery of radiation or systems with temperature controlled feedback. The flow of energy from the weld site into the surrounding tissue typically results in collateral thermal damage. This can occur in a region around the weld sites due to heat diffusion and cause an area of damage up to  $500\text{ }\mu\text{m}$  in width. Photodisruption can occur when laser power intensity is large enough to induce optical breakdown.<sup>31</sup> The high optical intensities required for photodisruption can be achieved at the focus of a high peak power fs laser beam.<sup>32,33</sup> Breakdown occurs only where the intensity is larger than the threshold level of the excited specimen.<sup>33</sup> Below this threshold level, the laser pulse passes through the material without causing damage. In earlier studies by Sacs et al., subsurface photodisruption of scleral tissue was achieved for the typical laser operating parameters of  $5\text{ }\mu\text{J}$  pulse energy at  $500\text{ fs}$ ,  $1064\text{ nm}$ , and a spot size on the order of  $5\text{ }\mu\text{m}$ .<sup>31</sup> The collateral thermal damage is reduced with the use of ultrashort-pulsed ps and fs lasers to weld tissue at a larger spot size. The concept of welding with ps and fs pulsed lasers is that the water in the collagen helix absorbs the pulse energy and is immediately raised to a much higher temperature than the surrounding tissue. This excitation breaks

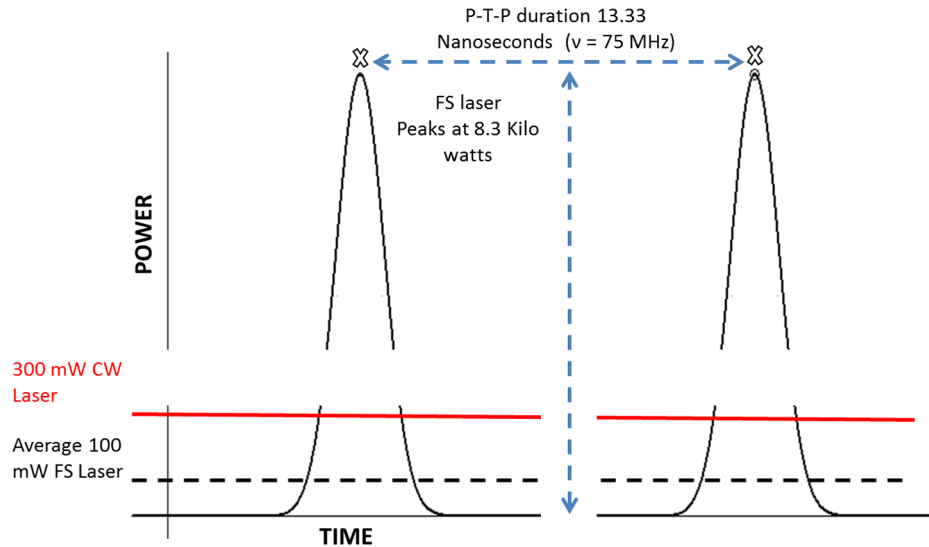


**Fig. 3** The nature and characteristics of CW (red) and fs (solid black) lasers used for the *in vivo* studies. The average power of fs laser is shown as black dash line. The diagram not to the scale.

the H<sub>2</sub>O mediated interchain and intrachain H bonds, hydrophobic interactions, and results in partial transient denaturing of the collagen (Figs. 1 and 2). As the intrachain and interchain molecular water cools, the hydrogen and other bonds are re-established in some of the renatured collagen helix (Figs. 1 and 2). Because the time between laser pulses is long compared to the pulse width, the average power can be lower than that for CW welding (see Fig. 3). Since the vibrational relaxation time of the water is less than the time between laser pulses, the water molecules have time to relax to the background tissue temperature. This can reduce the average tissue temperature and possibly reduce the extent of dehydration.

The vibrational overtone and combination mode absorption and vibrational relaxation time ( $T_1$ ) play a key role in renaturation of the collagen helix and thus can form high tensile strength laser welds. The laser wavelength and pulse duration are key parameters to investigate in order to form high tensile strength bonding. The optimum welding strength is achieved when the laser pulse width is less than the vibrational relaxation time,  $\sim 3$  ps, where the vibration states are pumped to higher levels before they have time to relax.<sup>14,15</sup> The mechanisms of laser-tissue interaction, depicted in Figs. 1, 2, 4, and 5 fall into two categories: (1) photothermal and (2) photochemical. It is important to note that the pulse energies that will be used in welding are on the order of 3 nJ/pulse for a fluence of 50  $\mu\text{J}/\text{cm}^2$  with an 80- $\mu\text{m}$  spot size. For comparison, the energy necessary for corneal ablation is 200  $\mu\text{J}$  in a 25  $\mu\text{m}$  spot for a fluence of 32  $\text{J}/\text{cm}^2$ .<sup>34,35</sup> Short fs and ps pulses favor the nonthermal modes depicted in Figs. 1, 4, and 5. The vibrational relaxation time,  $T_1$ , of O–H bonds in water (liquid phase) is on the order of 3 ps and is somewhat longer for bound water.<sup>36</sup> For long pulse or CW excitation, the vibration can relax within the pulse width and multiphoton processes are very weak. When the pulse width of the laser is on the order of or shorter than the vibrational relaxation time,  $< 3$  ps, the efficiency of multiphoton events is high and a significant fraction of the water molecules can be dissociated. It has been pointed out that for lower vibrational transitions in polyatomic molecules, the vibration and harmonicity could be nearly compensated by the rotational energy, so that the laser field could remain in near resonance with the rotation–vibration transitions between vibrational excited states.<sup>37–39</sup>

In polyatomic molecules, the density of vibrational states increases rapidly with energy because the large number of rotational and vibrational modes form a quasicontinuum.<sup>37–39</sup> One can expect efficient stepwise resonant or near resonant multiple phonon absorption to occur exciting the vibration from the ground state to a higher level.<sup>37,38</sup> If the coupling between modes is strong, the energy absorbed by the molecule in the quasicontinuum is expected to be distributed in all modes. With sufficient laser fluence, multiphoton and multiphoton absorptions can excite the molecule through the quasicontinuum into the true continuum above the dissociation threshold.<sup>37,38,40</sup> In addition, high-energy coherent radiation excites the molecules and atoms to an ionized state by the absorption of two or more photons by the chromophore at the same instance. This will result in a virtual excited state and further direct transition to an ionized state. The ionized moieties of chromophores get back to the ground state because of reformation of new electrostatic and covalent bonds (Fig. 1). In this situation, bound water in the collagen helix will achieve enough energy to dissociate and become highly mobile. As the water relaxes, the molecule can then reform bonds at a new location in the

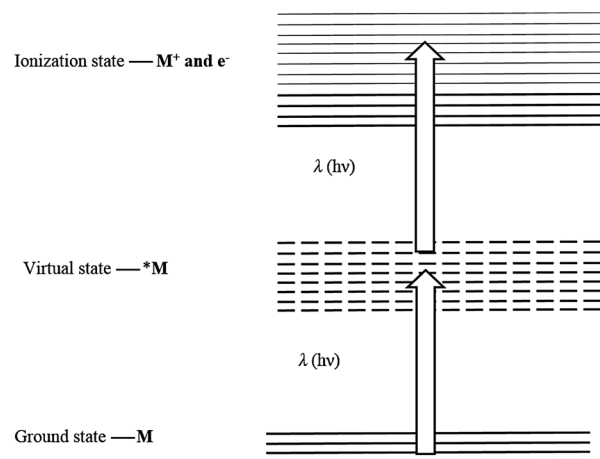


**Fig. 4** Basis for multiphoton absorption during fs laser tissue bonding and its effects on a chromophore.

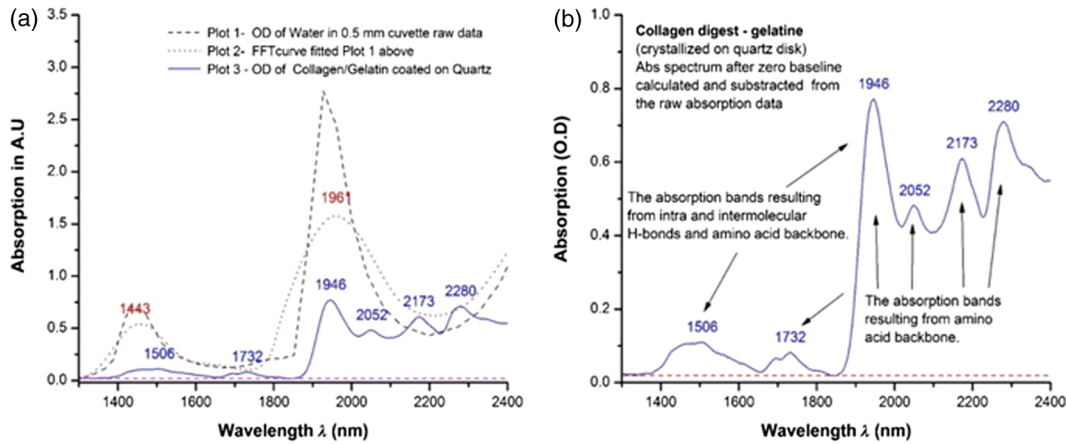


**Fig. 5** (a) NIR absorption spectra of dry gelatin (fragmented collagen) sample and water; (b) zero baseline calculated and subtracted spectrum derived from the raw spectrum of dried gelatin on a quartz disc showing absorption bands with their corresponding chromophore moieties.

helix. This energy may also be resonantly transferred to the other bonds. We find that using short pulses,  $\sim 100$  fs, at 1550 nm will give greater tensile strength in laser-welded tissue due to the involvement of bonds other than H bonds in this process. Pumping overtones and combination modes of water, collagen, and elastin causes better bonding. Using ultrafast laser pulses  $< 10$  ps make better welds and bonding with less damage.

Our earlier *ex vivo* animal tissue studies provided a variety of useful information related to various parameters involved in the development of LTB.<sup>29,30</sup> Successful welding requires precise control of laser power and exposure times to control the tissue temperature and dehydration. The principle parameters for the efficient fs NIR laser tissue bonding (LTB) and subsequent wound healing can only be discerned by carrying out investigations on living organisms because of the influences of physiological reactions of the body and functional elements involving constituent biochemical agents. Our *in vivo* studies on a guinea pig animal model enabled us to validate the new modality and helped in the extraction of essential parameters needed for pursuing *in vivo* clinical study on human subjects.

## 2 Materials and Methods

### 2.1 Absorption Spectroscopy

The absorbance of water in a 0.5 mm quartz cuvette and porcine skin collagen (90 bloom) dried on a quartz disc were measured by using Varian Cary 500 Scan UV/VIS/NIR spectrophotometer [Figs. 5(a) and 5(b)]. The absorption data were plotted using graphing and data analysis software OriginPro 7.0 (OriginLab Corporation, Northampton, Massachusetts).

### 2.2 In Vivo Guinea Pig Studies

All the protocols and animals used in this study were approved by Institutional Animal Care and Use Committee of City College of New York. A total of seven animals, female albino guinea pigs initially 7 to 8 weeks old with a weight of 400 to 500 g, were used in this study (Table 2).

#### 2.2.1 Laser surgical system

Two-lasers were used in this research. Figure 6 is the basic design of the laser welding system used in this study. The

first laser was an erbium fiber CW laser from B&W Tek model BWF2 (B&W Tek, Inc., Newark, Delaware) that emits at a wavelength of 1455 nm and has a maximum power level of 2 W. The emission wavelength of the erbium fiber laser in the NIR range corresponds to one of the absorption bands of water. The water absorption band peak occurs at 1450 nm from the combination of vibrations of (1,0,1). This absorption band covers a range from 1380 to 1600 nm. The second laser used for fs LTB studies was an IMRA femtoltile laser (IMRA America, Inc., Ann Arbor, Michigan) at 1550 nm; it was used at an average power of 100 mW.

The *in vivo* laser surgical system (Fig. 6) comprised of an animal surgical table and a laser beam fixed below the translational stage connected to a motion control system (Manufactured by Aerotech, Inc., Pittsburgh, Pennsylvania). The motion control system has the following components: a Unidex 500 PCI-based controller, a DR500 motor driver

**Table 2** Summary of study animals used for *in vivo* laser tissue welding in guinea pigs.

Animals	Type of weld	Laser power (mW)
GP0011	3 1450 CW	600
	1 Control suture	
GP0013-0014	5 IMRA welds	100
	1 CW weld	300
	2 control sutures	
GP0015-0016	6 CW welds	300
	2 Control sutures	
GP-0017 did not survive	IMRA	100
GP-0018	2 IMRA	90 IMRA
	1 CW	200 CW
	1 Control suture	

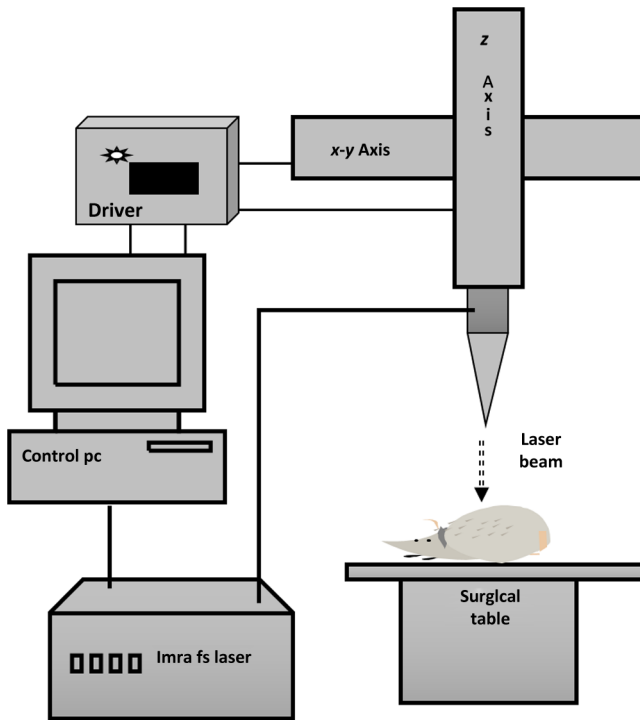


Fig. 6 The schematic of the *in vivo* laser surgical system setup.

and chassis, an ATS100-050 linear stepping motor, an ATS50-50 linear stepping motor, test software, and a software development kit, cables, and brackets. The function of the motion control system was to physically move the tissue under the laser beam in a pattern directed by the movement software. A Thorlabs MeterMate power meter (Thorlabs, Newton, New Jersey) was used to measure the laser power at the end of the objective lens prior to performing each of the tissue welds.

Guinea pigs are animals of choice because of their skin's similarity with human skin. The optimal wavelengths are 1455 and 1550 nm when ultrafast pulses (fs) are used. A fs IMRA fiber laser emitting at 1550 nm can be used to pump (1,0,1) modes of water.

The animals that were subjected to CW laser welding and pulse laser welding were euthanized on days 0, 2, 7, 21, and 42 as per the approved protocol using intraperitoneal injection of Euthasol® (pentobarbital sodium and phenytoin sodium) solution at a dose of 1 mL/kg bodyweight. The tissues were harvested immediately from the animals and either preserved for histological evaluation in 4% buffered formalin solution or immediately used for measuring the tensile strength of the welded tissues.

The tissues were routinely processed for histological sectioning. The 4  $\mu$  histological sections of the animal skin samples were stained with H&E and Masson's trichrome stain as per standard laboratory protocols.

### 3 Results

The histopathology of H&E and Masson's trichrome stained serial sections of *in vivo* laser welded skin tissues suggests that the use of CW and fs (IMRA) lasers at 90 to 100 mW power yielded better weld quality and postoperative healing. LTW resulted in minimal scar formation in the tissue when compared to the suture controls. The histological findings from this study are summarized in Table 2. The guinea pig GP0013 was euthanized on postoperative day 7 to evaluate the wound healing pattern and tissue regeneration. The sections of GP0013 [Figs. 7(a) and 7(b)] from the fs pulse laser welding show almost complete, near-normal reformation of the stratified squamous epithelium. The dermis shows active tissue regeneration of collagen fibrils and healthy granulation tissue. There is a minimal loss of dermal appendages along the line of the weld. The control sutured skin from the same animal [Figs. 8(a) and 8(b)] show poor healing, minimal granulation tissue, and more loss of dermal appendages. The late effects laser tissue welding

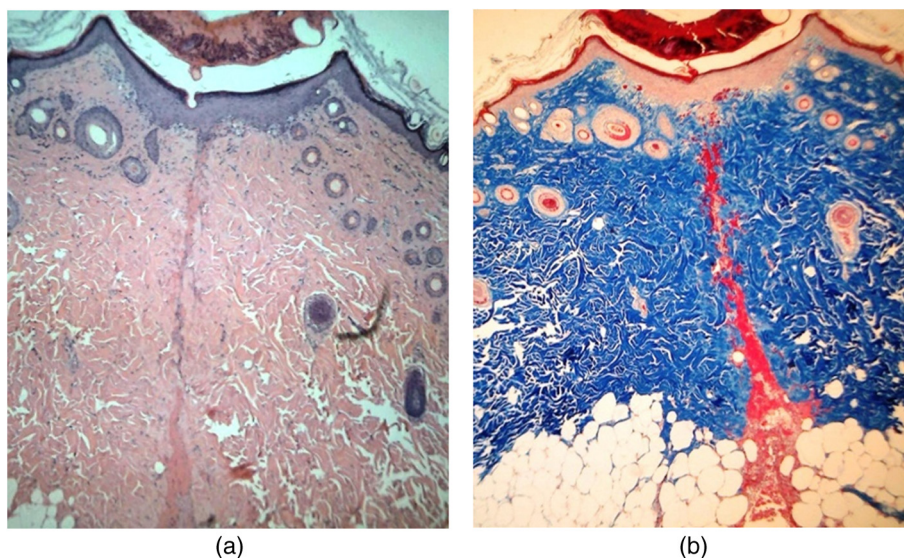
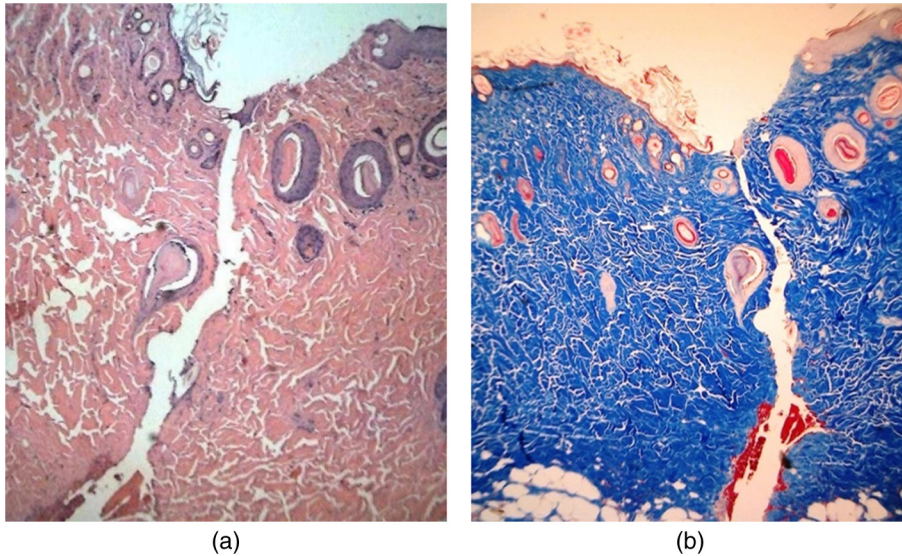


Fig. 7 (a) (H&E) and (b) (Masson's trichrome) 40 $\times$ : histology of 1550 nm fs laser welded *in vivo* skin samples of guinea pig GP 0013 after 7 postoperative days. The serial sections show a well-opposed surgical incision with almost complete wound healing in the epidermis, granulation tissue in the dermis, and no significant inflammatory cell infiltration.



**Fig. 8** (a) (H&E) and (b) (Masson's trichrome) 40x: histology of sutured control surgical incision of guinea pig GP0013 after 7 postoperative days. The serial sections show well-opposed surgical incision with very minimal wound healing in epidermis and minimal granulation tissue in dermis and no significant inflammatory cell infiltration.

evaluated in guinea pig GP0014 revealed minimal scar tissue formation and minimal loss of dermal appendages with laser welds than that of the control sutured tissues. The fs welds [Figs. 9(a) and 9(b)] have minimal residual effects of wound healing and a much better healing pattern than CW welded tissues [Figs. 10(a) and 10(b)]. Figure 11 shows the histology of a sutured incision on day 42, which showed epidermis with hyperkeratinized stratified squamous epithelium, extensive and irregular dermal collagen fiber deposition in dermis, and lack of hair follicles; there was no significant inflammatory cell infiltration. The guinea pigs shown in Figs. 12(a) and 12(b) were immediately postoperative and 42 days after CW and fs LTB.

The tissues grossly show minimal thermal effects in those welded with fs pulses lasers. Similar findings were observed after 80 postoperative days (Fig. 13).

#### 4 Discussion

The data of *in vivo* laser welding and animal wound healing histological evaluation are presented in Table 3. The results suggest that NIR pulse lasers (1550 nm) and low power CW lasers (1455 nm) may heal surgical wounds with less scar formation compared to the traditional sutures with silk. Low power fs and CW NIR use may assist in the prevention of keloid formation post operatively.

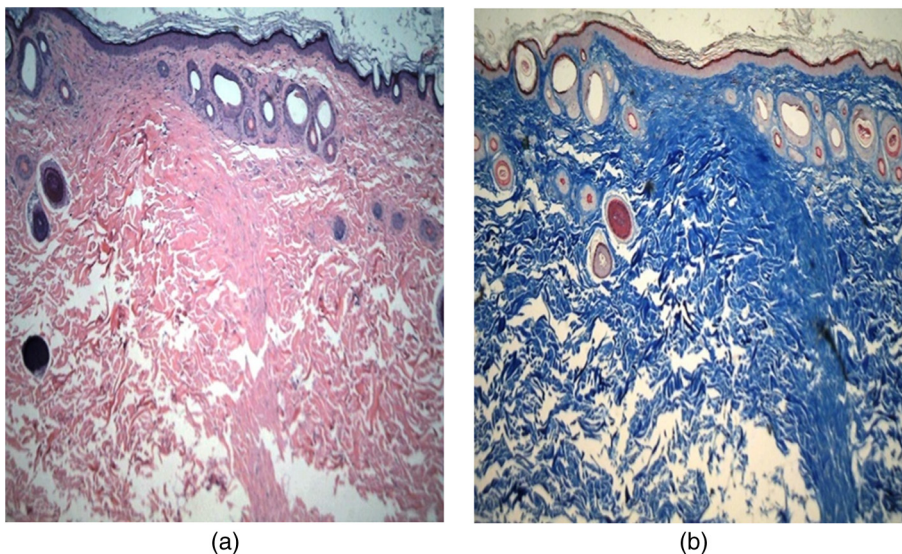


**Fig. 9** (a) (H&E) and (b) (Masson's trichrome) 40x: histology of fs IMRA surgical incision of guinea pig GP0014 after 42 postoperative days. The serial sections show fs IMRA laser at 1550 nm welded surgical incision wound healing in epidermis with almost normal stratified squamous epithelium and very minimal irregular collagen fiber deposition in dermis. The lack of hair follicles is confined only to the weld line, and there is no significant inflammatory cell infiltration.

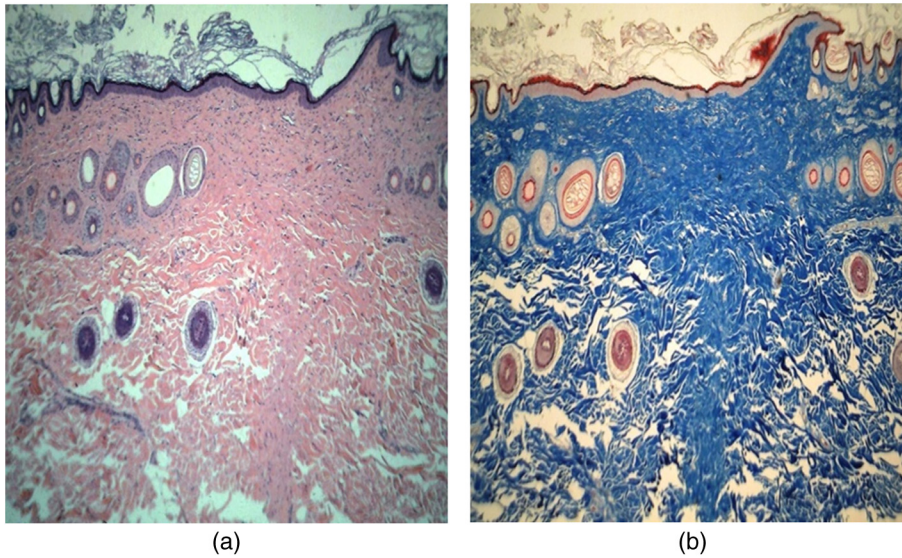


**Fig. 10** (a) (H&E) and (b) (Masson's trichrome) 40x: histology CW laser welded surgical incision of guinea pig GP0014 after 42 postoperative days. The serial sections show CW NIR laser at 1450 nm welded surgical incision wound healing in epidermis with almost normal stratified squamous epithelium and minimal irregular collagen fiber deposition in dermis. The lack of hair follicles is confined only to the weld line, and there is no significant inflammatory cell infiltration.

The key limitations for this study are weld time and wound dehiscence. The weld time is approximately 10 min for 1 cm of surgical incision using a single laser beam. However, the weld times can be decreased by using a multiple laser beam array. There was significant wound dehiscence, mostly partially in control and laser welded incisions up to 20% to 30% of the samples, which can be more attributable to the highly mobile nature of the animal that resulted in friction of the wound areas against the animal cage. Dehiscence may also be due to limited cross-linking of the collagen fibers as the fs NIR laser wavelength

used in this study is matched only to overtone absorption bands of specific tissue structural protein chromophores resulting in limited corresponding molecular cross-linking. To address this, an array of multiple laser beams with different wavelengths in the NIR range matched to different vibration bands and overtone vibrations may be used to achieve stronger tissue bonding with increased molecular cross-linking between various chromophores.

This study demonstrated the intrinsic chromophore molecular cross-linking of collagen and other structural proteins of

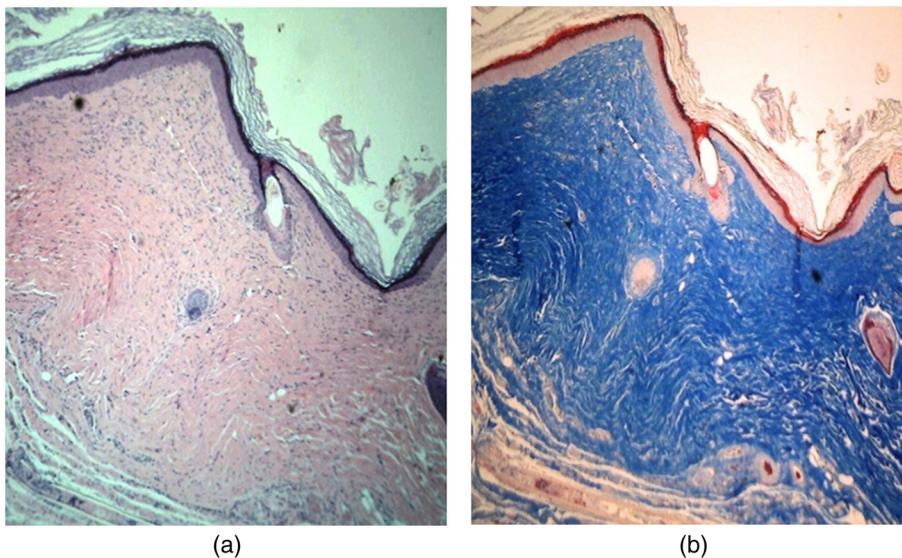


**Fig. 11** (a) (H&E) and (b) (Masson's trichrome) 40x: histology of sutured control surgical incision of guinea pig GP0014 after 42 postoperative days. The serial sections show control sutured surgical incision wound healing in epidermis with hyperkeratinized-stratified squamous epithelium and extensive and irregular dermal collagen fiber deposition in dermis, lack of hair follicles, and there is no significant inflammatory cell infiltration.

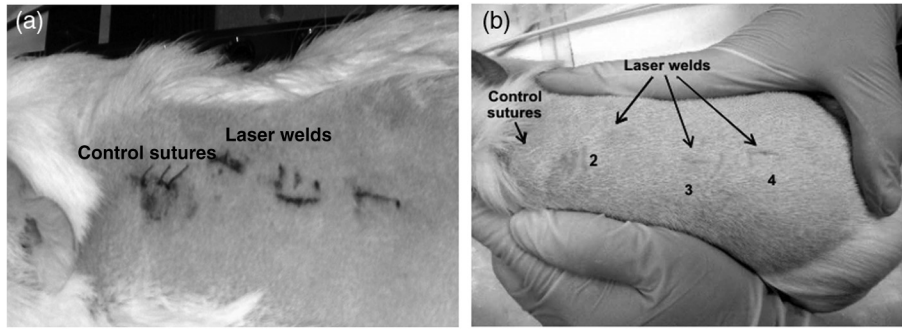


**Fig. 12** (a) *In vivo* guinea pig immediately after welding and (b) at 42 postoperative days. Incision 2 was welded with fs laser, incisions 3 and 4 with CW laser, and incision 1 was sutured.

**Table 3** The comparison of wound healing patterns and long-term residual tissue changes between control sutures, CW, and fs laser welds.

Features	Control (Figs. 8 and 11)	CW laser welds (Fig. 10)	Femtosecond laser weld (Figs. 7 and 9)
Wound healing pattern	<ol style="list-style-type: none"> <li>1. Very poor keratinized epithelium formation</li> <li>2. Relatively poor granulation tissue</li> <li>3. More extensive loss of dermal appendages</li> </ol>	<ol style="list-style-type: none"> <li>1. Reformation with reduced thickness of squamous epithelium</li> <li>2. Moderate loss of dermal appendages</li> </ol>	<ol style="list-style-type: none"> <li>1. Total reformation of keratinized squamous epithelium</li> <li>2. Healthy granulation tissue formation</li> <li>3. Minimally effected dermal appendages</li> </ol>
Residual tissue changes	<ol style="list-style-type: none"> <li>1. Hyperkeratosis, thickened epidermis</li> <li>2. Extensive collagen deposition in irregular pattern</li> <li>3. Irregular surface contours</li> <li>4. Extensive loss of dermal appendages</li> </ol>	<ol style="list-style-type: none"> <li>1. Near-normal epidermis, minimal hyperkeratosis</li> <li>2. Minimal collagen deposition</li> <li>3. Near-normal surface contour</li> <li>4. Minimal loss of dermal appendages</li> </ol>	<ol style="list-style-type: none"> <li>1. Almost normal epidermis, no hyperkeratosis</li> <li>2. Minimal collagen deposition, less irregular</li> <li>3. Normal surface contour</li> <li>4. Very minimal loss of dermal appendages</li> </ol>

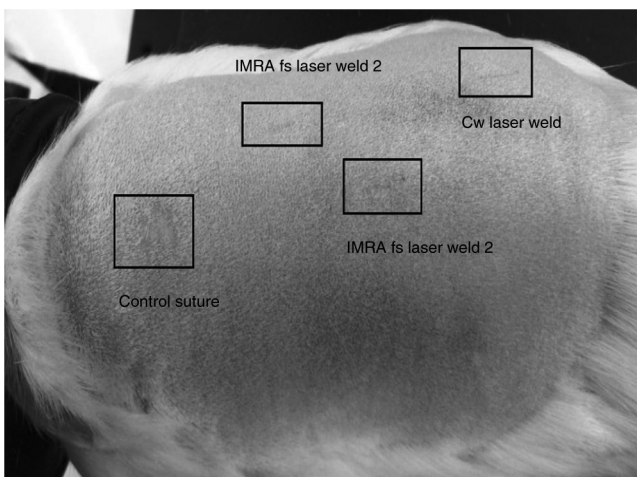


**Fig. 13** Guinea pig 80 days after tissue welding with fs (welds 1 and 2) and CW lasers. Scarring is less for the welded incisions than for the sutured incision.

biological tissues by using the fs NIR lasers tuned to vibrational overtones and combination modes of water molecules in tissue to match the overtones of water and collagen at NIR wavelengths. The property of nonlinear absorption is exhibited when molecules are subjected to very high-power coherent radiation sources such as fs laser pulses. The laser tissue welding using high-power coherent nonionizing laser radiation either CW or fs can induce certain biochemical and physiological responses at a molecular level in a living system that can induce tissue bonding as well as influence the wound healing processes and tissue architecture reorganization. It appears that laser radiations, both fs and CW, can alter inflammatory responses due to tissue injury by linear and nonlinear absorptions. The study showed distinct differences in wound healing patterns between CW laser and fs laser LTB, especially in the depth of penetration, the intensity of the inflammatory response, and the amount of collagen deposited at the site of wound closure. fs laser tissue welding compared to CW laser exhibits deeper penetration depths and bonding initiates in deeper tissues and progresses to superficial layers. The fs laser reduces the thermal damage

to living cells during LTB due to its nonthermal mechanisms of molecular cross-linking, and consequently reduces the post-surgical inflammatory response. The contrasting differences in wound healing pattern between CW and fs laser welds may possibly due to differing inflammatory and regeneration biomarker gene expression in the welded tissues. Therefore, multiphonon and multiphoton excitation with fs pulses offer the best condition for bonding live tissues followed by a better healing pattern. The ultrafast LTB offers an approach for surgical wound closure with reduced scarring and better wound healing.

### Acknowledgments

The authors would like to express their gratitude to the following individuals and agencies for kind support extended for this research work. We thank NIH for support under Grant No. RO1 EB000297-6. We thank the students Ms. Rakhi Podder, Ms. Nagmeh Davatgar, Mr. Rahul Chakraverty, Mr. Ronex Muthukatti, Ms. Sidra Piracha, and Ms. Shafika Elder for being very helpful during the experiments on this project at various stages. We thank Mr. Yury Budansky for help with building the LTB device. We thank Dr. Kestutis Sutkus of the Institute for Ultrafast Spectroscopy and Lasers, the City College of New York for very valuable help for the project and with preparation of this paper. We thank Professor Swapan Gayen, Professor Vladimir Petricevic of the Department of Physics at City College of New York, and Dr. Howard Savage of New York Eye and Ear Infirmary for being helpful in the management of this project at some stages and Dr. Alvin Katz for being involved in the early stage using CW lasers. Dr. Stephane Lubicz and Ms. Sabino Grech are involved with new ongoing LTW project. We thank Mr. Harry Acosta and his staff at Animal Facility at the City College of New York for very valuable help in the animal studies.

### References

1. L. S. Bass and M. R. Treat, "Laser tissue welding: a comprehensive review of current and future clinical applications," *Lasers Surg. Med.* **17**(4), 315 (1995).
2. J. Tang et al., "Tissue welding using near-infrared forsterite and cunyite tunable lasers," *IEEE J. Sel. Top. Quantum Electron.* **5**(4), 1103 (1999).
3. J. Tang et al., "A comparison of cunyite and forsterite NIR tunable laser tissue welding using native collagen fluorescence imaging," *J. Clin. Laser Med. Surg.* **18**(3), 117 (2000).
4. R. A. White et al., "Laser vascular welding—how does it work?" *Ann. Vasc. Surg.* **1**(4), 461 (1987).
5. D. S. Scherr and D. P. Poppas, "Laser tissue welding," *Urol. Clin. North Am.* **25**, 123 (1998).
6. J. Tang et al., "Morphological analysis of the microarterial media repair after 830 nm diode laser assisted end-to-end anastomosis, comparison with conventional manual suture," *Laser Med. Sci.* **12**, 300 (1997).
7. J. W. Verhoeven, "Glossary of terms used in photochemistry (IUPAC Recommendations 1996)," *Pure Appl. Chem.* **68**(12), 2223–2286 (2009).
8. N. M. Fried and J. T. Walsh Jr., "Laser skin welding: *in vivo* tensile strength and wound healing results," *Lasers Surg. Med.* **27**(1), 55 (2000).
9. M. E. Nimni, "Collagen, structure and function," in *Encyclopedia of Human Biology*, 2nd ed., Vol. **573**, Academic Press, New York (1997).
10. B. Brodsky and J. A. Ramshaw, "The collagen triple-helix structure," *Matrix Biol.* **15**(8–9), 545 (1997).
11. R. A. Berg and D. J. Prockop, "The thermal transition of a non-hydroxylated form of collagen. Evidence for a role for hydroxyproline in stabilizing the triple-helix of collagen," *Biochem. Biophys. Res. Commun.* **52**(1), 115 (1973).
12. G. Melacini et al., "Hydration dynamics of the collagen triple helix by NMR," *J. Mol. Biol.* **300**(5), 1041 (2000).
13. G. E. Chapman, S. S. Danyluk, and K. A. McLauchlan, "A model for collagen hydration," *Proc. R. Soc. B: Biol. Sci.* **178**(53), 465 (1971).
14. M. F. Kropman and H. J. Bakker, "Dynamics of water molecules in aqueous solvation shells," *Science* **291**(5511), 2118 (2001).
15. M. F. Kropman, H. K. Nienhuys, and H. J. Bakker, "Real-time measurement of the orientational dynamics of aqueous solvation shells in bulk liquid water," *Phys. Rev. Lett.* **88**(7), 077601 (2002).
16. S. K. Holmgren et al., "Code for collagen's stability deciphered," *Nature* **392**(6677), 666 (1998).
17. S. K. Holmgren et al., "A hyperstable collagen mimic," *Chem. Biol.* **6**(2), 63 (1999).
18. J. Bella et al., "Crystal and molecular structure of a collagen like peptide at 1.9 Å resolution," *Science* **266**(5182), 75 (1994).
19. M. G. Venugopal et al., "Electrostatic interactions in collagen-like triple-helical peptides," *Biochemistry* **33**(25), 7948–7956 (1994).
20. J. Engel et al., "The triple helix in equilibrium with coil conversion of collagen-like polytripeptides in aqueous and nonaqueous solvents. Comparison of the thermodynamic parameters and the binding of water to (L-Pro-L-Pro-Gly)<sub>n</sub> and (L-Pro-L-Hyp-Gly)<sub>n</sub>," *Biopolymers* **16**(3), 601 (1977).
21. I. Ojima, J. R. McCarthy, and J. T. Welch, *Biomedical Frontiers of Fluorine Chemistry*, American Chemical Society, Washington, DC (1996).
22. N. Panasik, Jr. et al., "Inductive effects on the structure of proline residues," *Int. J. Pept. Protein Res.* **44**(3), 262 (1994).
23. E. S. Eberhardt, N. Panasik, Jr., and R. T. Raines, "Inductive effects on the energetics of prolyl peptide bond isomerization: implications for collagen folding and stability," *J. Am. Chem. Soc.* **118**(49), 12261 (1996).
24. J. J. Baraga, M. S. Feld, and R. P. Rava, "In situ optical histochemistry of human artery using near infrared Fourier transform Raman spectroscopy," *Proc. Natl. Acad. Sci. U. S. A.* **89**(8), 3473 (1992).
25. M. S. Feld, "Laser Raman spectrum of calcified human aorta," *Lasers Surg. Med.* **12**, 552 (1992).
26. C. H. Liu et al., "Near-IR Fourier transform Raman spectroscopy of normal and atherosclerotic human aorta," *Lasers Life Sci.* **4**, 257 (1992).
27. R. Manoharan et al., "Quantitative histochemical analysis of human artery using Raman spectroscopy," *J. Photochem. Photobiol. B* **16**, 211 (1992).
28. H. Susi, J. S. Ard, and R. J. Carroll, "The infrared spectrum and water binding of collagen as a function of relative humidity," *Biopolymers* **10**, 1597–1604 (1971).
29. V. Sriramoju et al., "Alfano RR management of heat in laser tissue welding using NIR cover window material," *Lasers Surg. Med.* **43**(10), 991–997 (2011).
30. V. Sriramoju and R. R. Alfano, "Laser tissue welding analyzed using fluorescence Stokes shift spectroscopy and Huang–Rhys parameter," *J. Biophotonics* **5**(2), 185–193 (2012) [Epub 2011 Nov 11].
31. Z. S. Sacs et al., "Subsurface photodisruption inhuman sclera: wavelength dependence," *Ophthalmic Surg. Lasers Imaging* **34**, 104 (2003).
32. R. R. Anderson and J. A. Parrish, "Selective photothermolysis: precise microsurgery by selective absorption of pulsed radiation," *Science* **220**, 524 (1983).
33. J. A. Parrish et al., "Selective thermal effects with pulsed irradiation from lasers: from organ to organelle," *J. Invest. Dermatol.* **80**(Suppl.), 75s (1983).
34. S. Leikin et al., "Raman spectral evidence for hydration forces between collagen triple helices," *Proc. Natl. Acad. Sci. U. S. A.* **94**(21), 11312 (1997).
35. D. Stern et al., "Corneal ablation by nanosecond, picosecond, and femtosecond lasers at 532 and 625 nm," *Arch. Ophthalmol.* **107**, 587 (1989).
36. S. Woutersen et al., "Anomalous temperature dependence of vibrational lifetimes in water and ice," *Phys. Rev. Lett.* **81**, 1106 (1998).
37. D. M. Larsen and N. Bloembergen, "Excitation of polyatomic molecules by radiation," *Opt. Commun.* **17**, 254 (1976).
38. N. Bloembergen, "Comments on the dissociation of polyatomic molecules by intense 10.6 μm radiation," *Opt. Commun.* **15**, 416 (1975).
39. R. R. Alfano and S. L. Shapiro, "Establishment of a molecular-vibration decay route in a liquid," *Phys. Rev. Lett.* **29**, 1655 (1972).

40. S. J. Chung et al., "Cooperative enhancement of two-photon absorption in multi-branched structures," *J. Phys. Chem. B* **103**(49), 10741–10745 (1999).

**Vidyasagar Sriramoju** is a physician scientist received medical degree and postgraduate training from Osmania Medical College, India (1985 to 1996). He worked at the City College of New York, CUNY as a postdoctoral researcher initially in neurobiology (2002 to 2004) and later at the Institute for Ultrafast Spectroscopy and Lasers (2004 to 2010). Earlier he worked as a researcher at the

Pennsylvania State University (1999 to 2001) and as a pathologist in India (1996 to 1998).

**Robert R. Alfano** is a distinguished professor of science and engineering at the City College of CUNY, where he has been a faculty member in the Department of Physics since 1972. Prior to joining the City College, he was a research physicist at the GTE Research Laboratories from 1964 to 1972. He received his PhD in physics from New York University in 1972. He is a director of the CCNY Institute of Ultrafast Spectroscopy and Lasers.